Harmonic Phase Shifter for Discrete Amplitude Modulation Technique

Dr. Anas Lateef Mahmood
Electronic and Communications Engineering Department
Nahrain University, College of Engineering,
Anaslatif_78@yahoo.com

Dr. Mohammed Tofik Lazim
Philadelphia University, Department of Electrical Engineering, Jordan
drmohamadtofik@yahoo.com

Abstract

In discrete amplitude modulation or integral-cycle control, subharmonic and higher order harmonic components are generated in the three phases of a three − phase system. These harmonic components are found to be unbalanced in phase displacement. The correction of the unbalanced phase displacement angles of a particular subharmonic or higher order harmonic for this type of triggering is investigated to solve the limitation of use of this important type of control as a drive and many other industrial applications. The multiple of 2π phase shifting technique is used to correct unbalanced phase displacement angles produced in a three-phase system. A computer-based harmonic phase corrector is designed and tested with three-phase resistive and induction motor loads. It is found that there is a well agreement between the theoretical and experimental results and it is believed that the major problems associated with the integral-cycle triggering mode with three-phase circuits have been solved in the present work.

key words: Harmonics, integral cycle control, power electronics, phase angle correction, phase shifter

I. Introduction

Load voltage control by means of switching a pair of inverse parallel connected thyristors or triac is well established. It is customary to use modes of thyristor triggering known as integral-cycle triggering whereby burst of complete cycles of current are followed by complete cycles of extinction [1-4].

Integral-cycle triggering results in conduction patterns that contain subharmonics of the supply frequency and so constitute a form of step-down frequency changing that can be considered as a form of frequency changer. Also integral-cycle triggering results in a considerable reduction in the amplitudes of the higher order harmonics as compared with other triggering techniques and it is possible that Radio Frequency Interference (RFI) is negligible [2]. The phase-control switching can produce higher order harmonics and heavy inrush current while switching on in a cold start [5], while integral-cycle control circuits have the advantage of low inrush current due to zero voltage switching ease in construction and low hardware cost. Therefore, integral-cycle control loads have been widely used in resistive loads, such as heaters, oven, furnaces, and spot welders [6-8]. Also it is used in speed control of single-phase induction motor and dc series motor [9-10].

As a frequency changing scheme, integral-cycle triggering was found not feasible for applications in the three-phase systems exploiting this technique for ac motor speed control [11]. This is because the amplitudes and phase displacement angles of the higher order harmonic and subharmonic components of the integral-cycle controlled waveform are determined by the conduction period N and the control period T and the order of the individual harmonic. The three-phase analysis of voltage and current waveforms and phase relationships of the generated harmonic and subharmonic components for different circuit configurations are described [12-13].

Consider a three-phase resistive load with line voltage control as shown in Fig. 1. The resulting three-load voltage waveforms are identical and so are the three-load current waveforms. The supply frequency components are found to be balanced, since they are 120º apart in time-phase while the phase displacement angles of a particular subharmonic or higher order harmonic are unbalanced [11, 12]. Due to the unbalanced phase relationships of the subharmonic components, these components represent a source of trouble when these voltage waveforms are used to feed ac machines for speed control purposes [11]. In this paper an attempt is made to study the phase unbalanced characteristics of the subharmonics as well as the higher order harmonics generated due to integral-cycle triggering, and a new phase shifting technique is found that is capable of correcting the unbalanced phases based on microprocessor implementation [14].
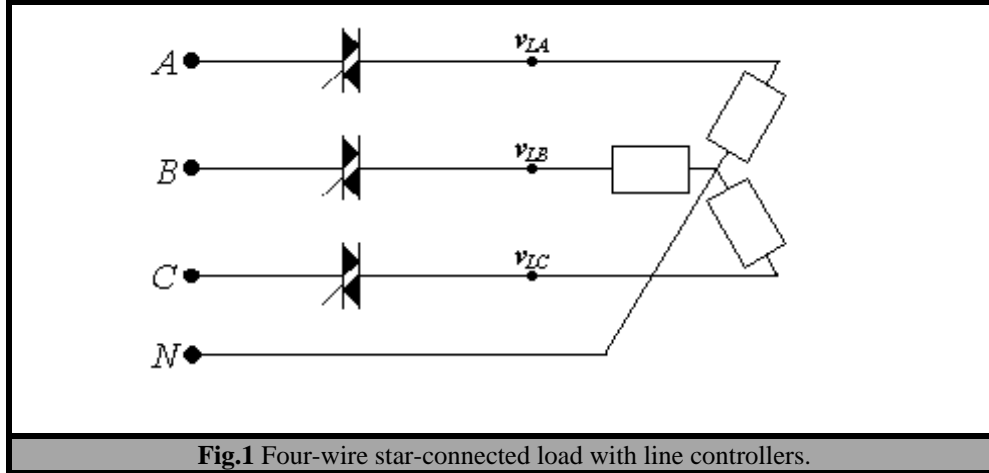
Fig.1 Four-wire star-connected load with line controllers.

II. The Proposed Phase Shifting Technique

Fig. 2 depicts the waveforms of the load voltages for the case when using integral-cycle control with control period $T = 2$ and conduction period $N = 1$, for the circuit shown in Fig. 1 with R-L load. Let the notation 1, 2, 3 denote the three phases A, B, and C respectively. Thus the load voltage (v_{Lj}) for any j^{th} phase will have the general form [12].

$$v_{Lj} = \sqrt{2}V\sin\left(\omega Tt - \gamma_j\right) \qquad \frac{\gamma_j}{T} \leq \omega t \leq \frac{2\pi N + \phi + \gamma_j}{T} \qquad \boxed{1}$$

$j = 1, 2, 3$

$\gamma_1 = 0, \quad \gamma_2 = 2\pi/3, \quad \gamma_3 = 4\pi/3$

$\phi = \tan^{-1}\dfrac{\omega L}{R}$

Fourier analysis of Eq. (1) results in the following mathematical expressions:

for $n \neq T$, the dc component is

$$a_0 = \frac{\sqrt{2}V}{\pi T}\left[1 - \cos\phi\right] \qquad \boxed{2}$$

The amplitude c_n of nth order subharmonic or higher order harmonic as well as its phase displacement ψ_n are found as follows.

$$a_{nj} = \frac{\sqrt{2}V}{\pi\left(T^2 - n^2\right)}\left[T\left\{\begin{array}{l}\cos\dfrac{n\gamma_j}{T} - \cos\phi\cos\\ \dfrac{n}{T}\left(2\pi N + \phi + \gamma_j\right)\end{array}\right\} - n\sin\phi\sin\dfrac{n}{T}\left(2\pi + \phi + \gamma_j\right)\right] \qquad \boxed{3}$$

$$b_{nj} = \frac{\sqrt{2}V}{\pi\left(T^2 - n^2\right)}\left[T\left\{\begin{array}{l}\sin\dfrac{n\gamma_j}{T} - \cos\phi\sin\\ \dfrac{n}{T}\left(2\pi N + \phi + \gamma_j\right)\end{array}\right\} + n\sin\phi\cos\dfrac{n}{T}\left(2\pi + \phi + \gamma_j\right)\right] \qquad \boxed{4}$$

$c_{nj} = \sqrt{a_{nj}{}^2 + b_{nj}{}^2}$

$$c_{nj} = \frac{\sqrt{2}V}{\pi\left(T^2 - n^2\right)}\left[T^2\left\{\begin{array}{l}\cos\dfrac{n}{T}\left(2\pi N + \phi\right)\\ -\cos\phi\end{array}\right\}^2 + \left\{\begin{array}{l}T\sin\dfrac{n}{T}\left(2\pi N + \phi\right)\\ -n\sin\phi\end{array}\right\}^2\right]^{1/2} \qquad \boxed{5}$$

$\psi_{nj} = \tan^{-1}\dfrac{b_{nj}}{a_{nj}}$

$$\psi_{nj} = \tan^{-1}\frac{T\left\{\begin{array}{l}\cos\dfrac{n\gamma_j}{T} - \cos\phi\cos\\ \dfrac{n}{T}\left(2\pi N + \phi + \gamma_j\right)\end{array}\right\} - n\sin\phi\sin\dfrac{n}{T}\left(2\pi + \phi + \gamma_j\right)}{T\left\{\begin{array}{l}\sin\dfrac{n\gamma_j}{T} - \cos\phi\sin\\ \dfrac{n}{T}\left(2\pi N + \phi + \gamma_j\right)\end{array}\right\} + n\sin\phi\cos\dfrac{n}{T}\left(2\pi + \phi + \gamma_j\right)} \qquad \boxed{6}$$

For the supply frequency component, the Fourier coefficients are

$$a_{Tj} = \frac{\sqrt{2}V}{4\pi T}\left[\begin{array}{l}\cos\gamma_j - 2\left(2\pi N + \phi\right)\sin\gamma_j\\ -\cos\left(2\phi + \gamma_j\right)\end{array}\right] \qquad \boxed{7}$$

$$b_{Tj} = \frac{\sqrt{2}V}{4\pi T}\left[\begin{array}{l}\sin\gamma_j + 2\left(2\pi N + \phi\right)\cos\gamma_j\\ -\sin\left(2\phi + \gamma_j\right)\end{array}\right] \qquad \boxed{8}$$

$$c_{Tj} = \frac{\sqrt{2}V}{4\pi T}\left[\begin{array}{l}2\left(1 - \cos 2\phi\right) + 4\left(2\pi N + \phi\right)\\ \left(2\pi N + \phi - \sin 2\phi\right)\end{array}\right]^{1/2} \qquad \boxed{9}$$

$$\psi_{nj} = \tan^{-1} \frac{b_{nj}}{a_{nj}} \qquad \boxed{10}$$

It is found in [15] that the nth frequency component of load current in phase A (ψ_{n1}) leads that of phase B (ψ_{n2}) by $120^o \frac{n}{T}$ and (ψ_{n2}) leads (ψ_{n3}) by $120^o \frac{n}{T}$ also. However, if the phase displacement of the jth phase (γ_j) is shifted according to the following relationship

$$\gamma_j = \gamma_j' + 2\pi m_j \qquad \boxed{11}$$

where γ_j represent the new shifting angle, and

$m_j = 1, 2 \ldots T\text{-}1$.

$m_1 = 0$, $\gamma_1' = 0$, $\gamma_2' = 2\pi/3$, and $\gamma_3' = 4\pi/3$

This new value of γ_j do not affect the amplitude and phase angle relationships of the supply frequency components at the load voltages. It can be seen from Eq. (5), that the amplitude of the nth harmonic is independent of γ_j, which means that, the variation of γ_j does not affect the harmonic amplitude spectrum of the jth phase. Only the phase displacement angle ψ_n of the nth harmonic is changed as could be seen from Eq. (6). The phase displacement angle ψ_{nj} of the nth harmonic varies with the variation of m_j.

Now after shifting the load voltage waveform of phase B or C or both of them by multiple of 2π the nth frequency component of load current in phase A (ψ_{n1}) leads that of phase B (ψ_{n2}) by

$$(120^O + 360^O \times m_2)\frac{n}{T} \qquad \boxed{12}$$

and (ψ_{n1}) leads (ψ_{n3}) by

$$(240^O + 360^O \times m_3)\frac{n}{T} \qquad \boxed{13}$$

The harmonic amplitude spectrum and the phase angle relationships for the load voltage waveforms of Fig. 2 are depicted in Figs. 3 and 4 respectively. It is seen that, the phase displacement angles of the subharmonics and the higher order harmonics are unbalanced. Now, if the phase displacement angle of phase B, i.e. ψ_{n2}, is shifted by 180° then the phase displacement angles of the 1st harmonic (25Hz) and the 5th harmonic (125Hz), as for example, become balanced.

The new values of ψ_{n2} for the 1st, 3rd, and 5th harmonics which are $\psi_{12} = 210^o$, $\psi_{32} = 270^o$, and $\psi_{52} = 150^o$ respectively give the value $m_2 = 1$, and the new value of γ_2 is equal to 480°. When γ_2 equal to 480° the harmonic amplitude spectrum and the phase displacement angles of the supply frequency component remains unchanged, while the phase displacement angles of the 1st, 3rd, and 5th harmonics changed as shown in Fig. 5(a), (c), and (d) respectively. It is found that this shifting

Fig 2 Typical load voltages for phases A, B, and C
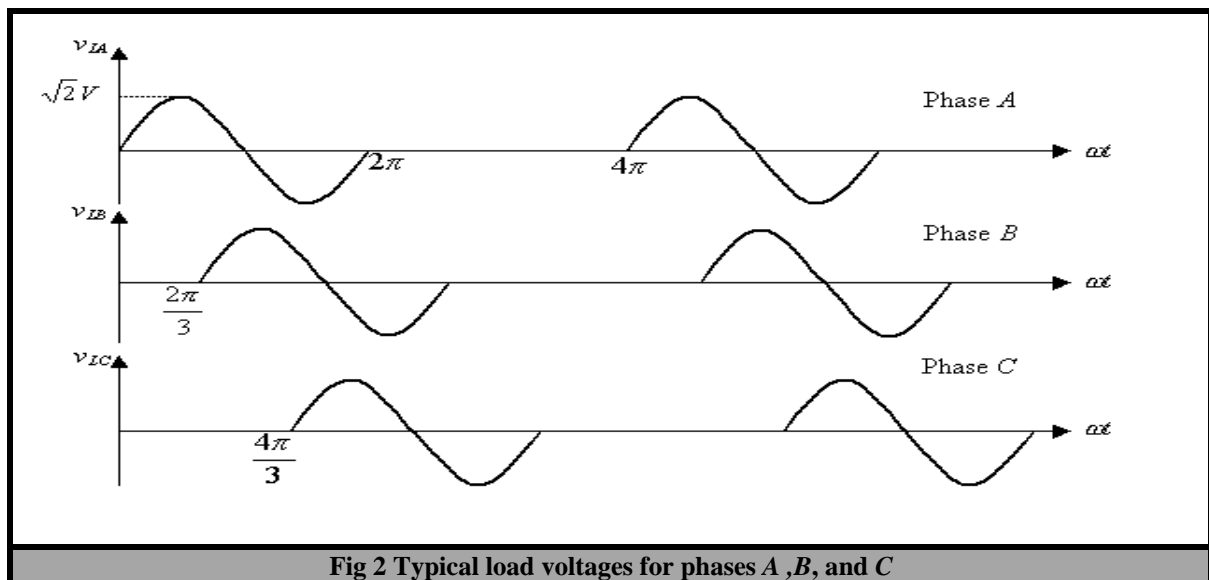
technique makes the phase displacement angles of the nth harmonic order balanced (120° between the phases) except when n is a multiple of 3 where in this case the phase displacement angles become in phase for all values of N and T except when T is a multiple of 3. Also it is noticed that the phase shifting of the phase displacement angles used in this technique do not depend on the value of N. This means that, the values of γ_2 and γ_3 that makes n^{th} order harmonic balanced for certain values of N and T can make it balanced as well for the same value of T with $N = N$-1, N-2, …, 1. Table (1) shows the values of m_2 and m_3 which make the phase displacement angles of the nth harmonic either balanced or in phase for typical values of T and N. This technique cannot correct the phase displacement angles of a particular subharmonic or higher order harmonic if T is a multiple of 3.

Table (1)			
T	N	m_2	m_3
2	1	1	0
4	3 – 1	1	2
5	4 – 1	3	1
7	6 – 1	2	4
8	7 – 1	5	2
10	9 – 1	3	6

III. Practical Implementation

The schematic diagram of the microprocessor-based harmonic phase shifter for integral-cycle control is shown in Fig. 6. After reducing the three-phase supply voltage by the step-down transformers (T1, T2, and T3), the zero crossing detector (ZCD) circuits produces the 180°-degree pulses to an 8085 microprocessor-based system. The microprocessor now can sense the zero-instant of the ac supply. Then the conduction of the triacs started by sending high pulses to the gate drive circuits (the gate drive circuit used from [16]). The output of each gate drive circuit is

connected to pulse transformers (T4, T5, and T6), that are used to isolate the microprocessor circuit from the power circuit. In order to ensure successful triggering of the triac, the trigger voltage must be maintained for the entire conduction period. This can be achieved by using a square pulses at high frequency and these pulses are generated by the timing circuit. A NAND gate is used to modulate the higher frequency pulses with the main conduction pulse.

Fig. 7 shows the signals at different stages in the control circuit for phase A programmed for a conduction period of 1 cycle out of two. The square pulse E goes through a buffer circuit that is found necessary for the elimination of the dc bias generated in the comparator. The microprocessor sends a square pulses through port PB0 of the 8155 with ON/OFF ratio equal to N/(T-N).
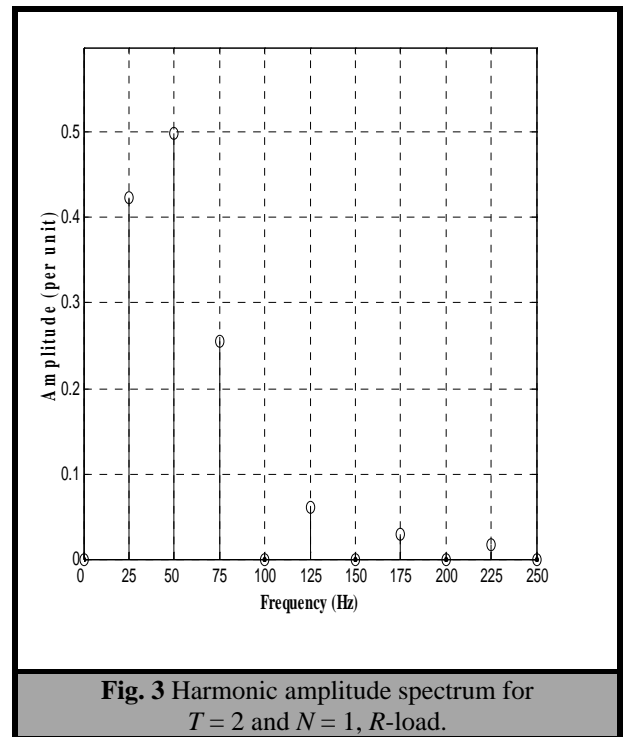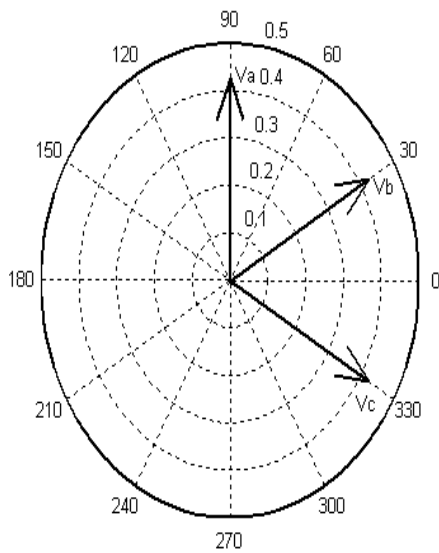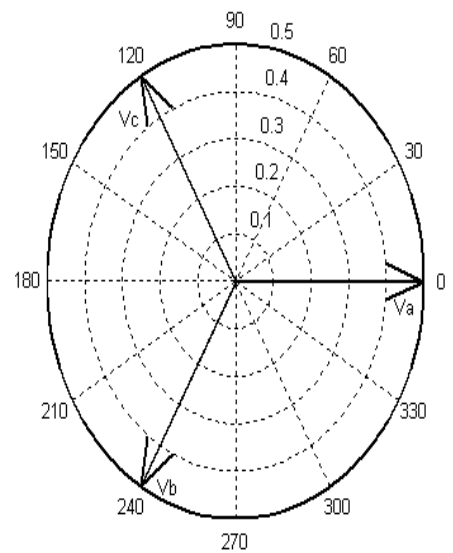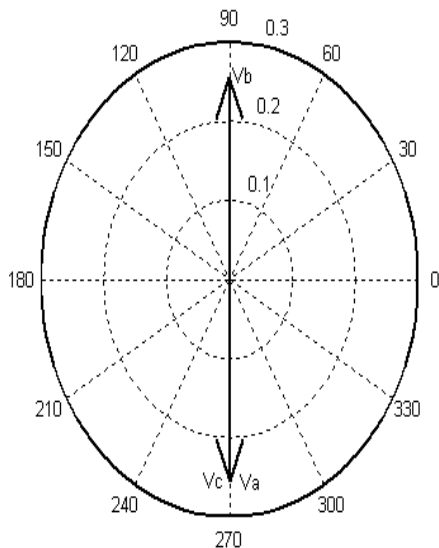

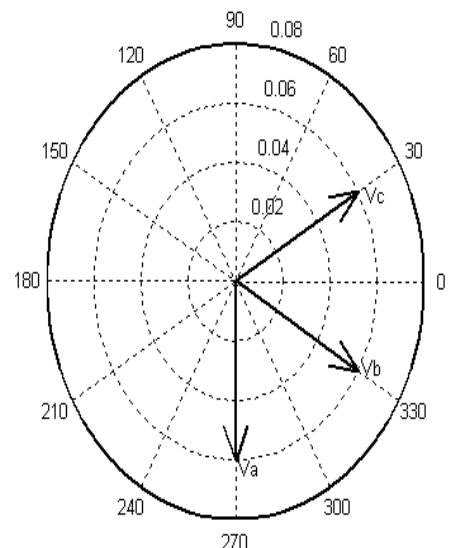**Fig. 3** Harmonic amplitude spectrum for $T = 2$ and $N = 1$, R-load.

(a)

(b)

(c)

(d)

Fig. 4 Phase displacement angles for $T = 2$ **and** $N = 1$, R**-load (a) 1**st **harmonic (25Hz) Vb (-60**^{o}**) Vc (-120**^{o}**) (b) supply frequency component Vb (-120**^{o}**) Vc (-240**^{o}**) (c) 3**rd **harmonic (75Hz) Vb (-180**^{o}**) Vc (-360**^{o}**) (d) 5**th **harmonic (125Hz). Vb (-300**^{o}**) Vc (-240**^{o}**)**

Fig. 5 Phase displacement angles for $T = 2$ and $N = 1$, R-load (a) 1st harmonic (25Hz) (b) supply frequency component (50Hz) (c) 3rd harmonic (75Hz) (d) 5th harmonic (125Hz)

The output of each gate drive circuit is connected to pulse transformers (T4, T5, and T6), that are used to isolate the microprocessor circuit from the power circuit. In order to ensure successful triggering of the triac the trigger voltage must be maintained for the entire conduction period. This can be achieved by using a square pulses at high frequency and these pulses are generated by the timing circuit. A NAND gate is used to modulate the higher frequency pulses with the main conduction pulse.

Fig. 7 shows the signals at different stages in the control circuit for phase A programmed for a conduction period of 1 cycle out of two. The square pulse E goes through a buffer circuit that is found necessary for the elimination of the dc bias generated in the comparator. The microprocessor sends a square pulses through PB0 of the 8155 with ON/OFF ratio equal to $N/(T-N)$.

IV. Experimental Results

The control circuit shown in Fig. 6 was built and tested in the laboratory with a three-phase balanced resistive load. Fig. 8 shows oscillograms of the load voltage waveforms v_{LA}, v_{LB}, and v_{LC} for the case when $T = 4$ and $N = 2$ before and after

the application of the phase-shifting technique while Fig. 9 shows the harmonic amplitude spectrum.

The system was tested also with a three-phase, cage-type induction motor described in Appendix A. The stator windings were connected in 4-wire, star-connected form. Practically this type of voltage control, i.e. integral-cycle, is found to produce some problems to the motor such as noise, vibration, and heat rising to the motor windings. These problems become severe especially at high voltages and when the motor runs continuously. However, table 2 shows the speed measurement of the motor at different values of N and T using a digital tachometer before and after the phase displacement angles correction in addition with the frequency of rotation for each case that is calculated using the following equation of the three-phase induction motor speed [17]:

$$ n_s = 120\frac{f}{p} \qquad 14 $$

where p = number of poles and f = supply frequency.

It is important to mention that the motor rotates in the reverse direction for some cases after the correction of the phase displacement angles and this is due to the variation in the phase sequence after the correction of the phase displacement angles.

However, these results show that, the motor speed n_s is changed after the correction of the phase displacement angles. This is because the phase displacement angles of the first harmonic become balanced, i.e. separated by 120° in time phase, and it will produce its own speed. This means that *"after the correction of the phase displacement angles of the first harmonic, the motor began to rotate at the desired subharmonic frequency"*.

The three-phase induction motor is loaded by a dc dynamometer available in the laboratory to examine the performance of the motor under load condition. The dc dynamometer is connected as a separately excited machine as shown in Fig. 10. The specifications of the 3-phase motor and the dynamometer (found in Machines laboratory, Electronic and Communications Department, Nahrain University) are given in Appendix B. The field winding of the dynamometer is connected to a 220V dc source and the field current is set to the maximum permissible value.
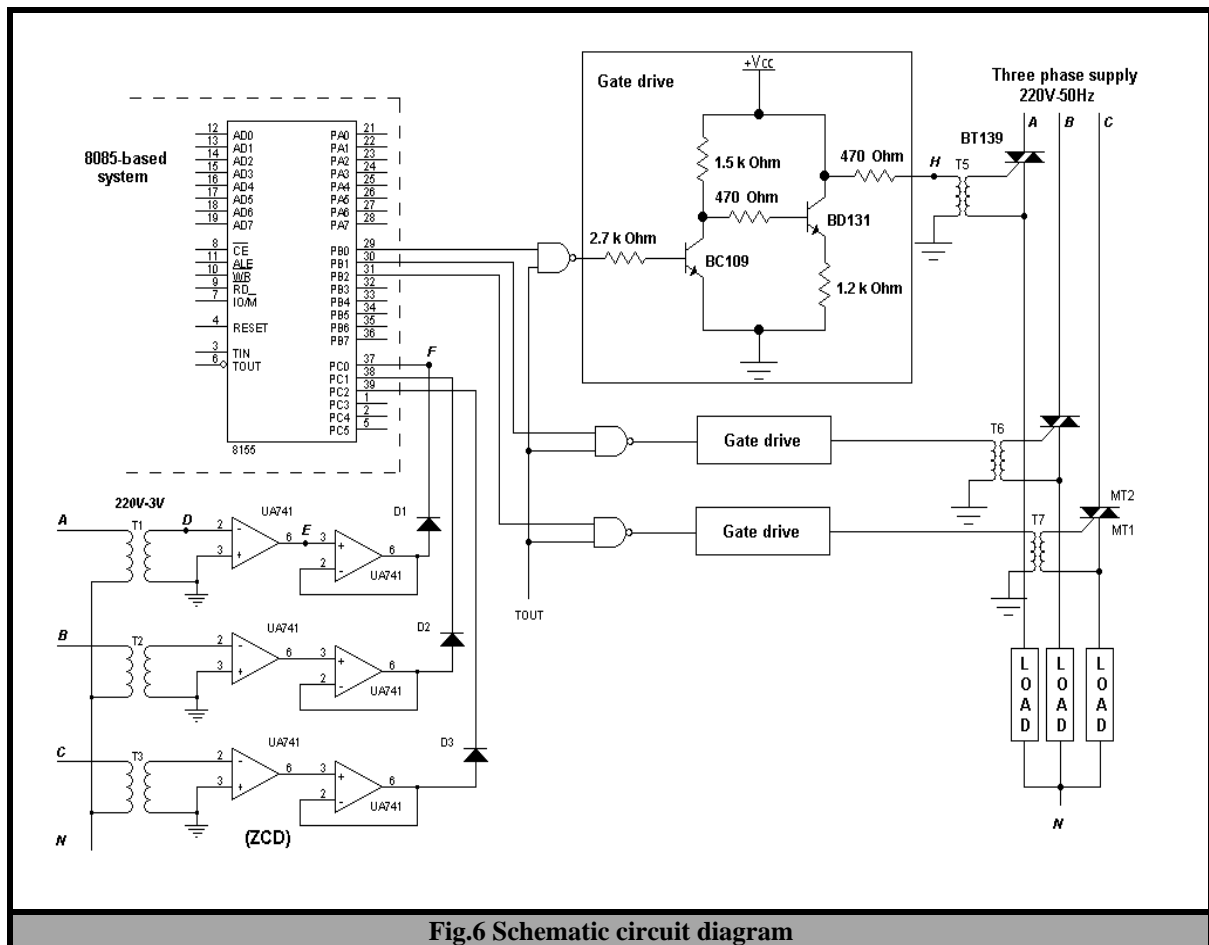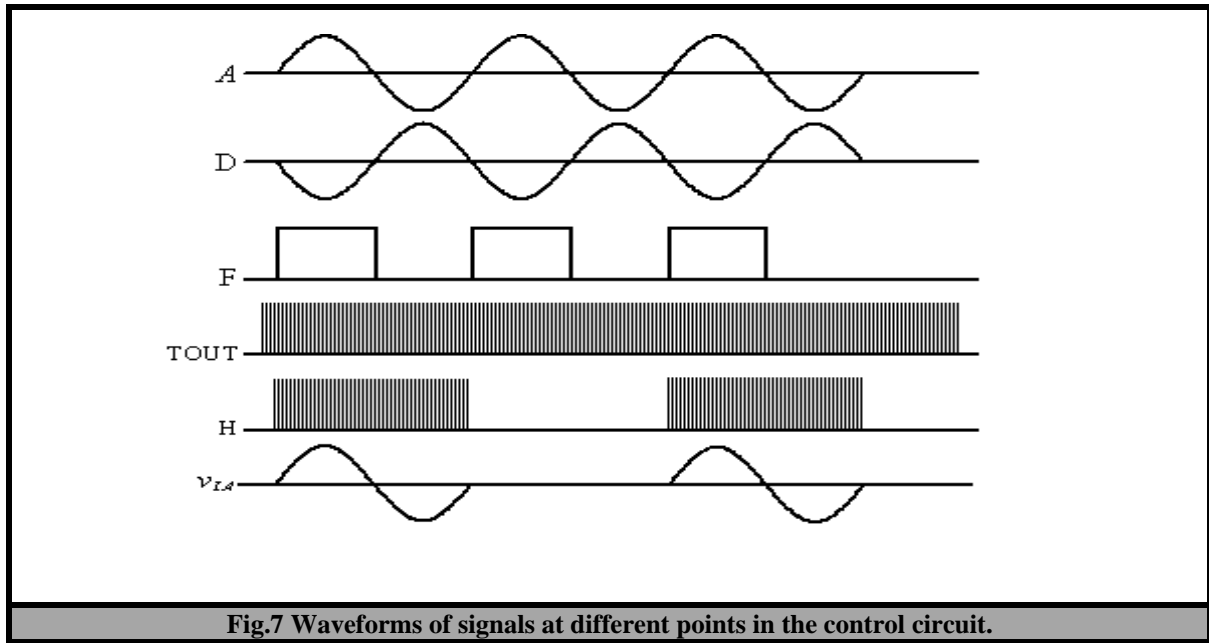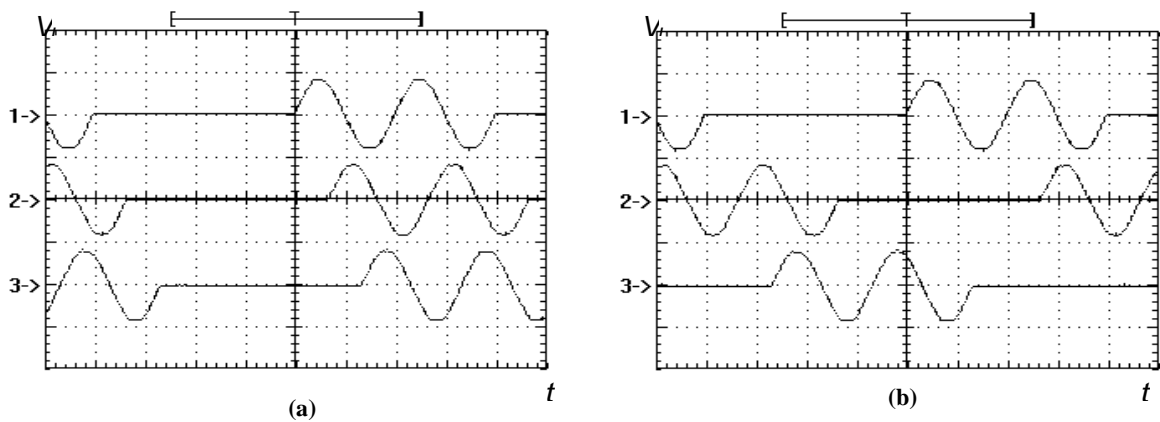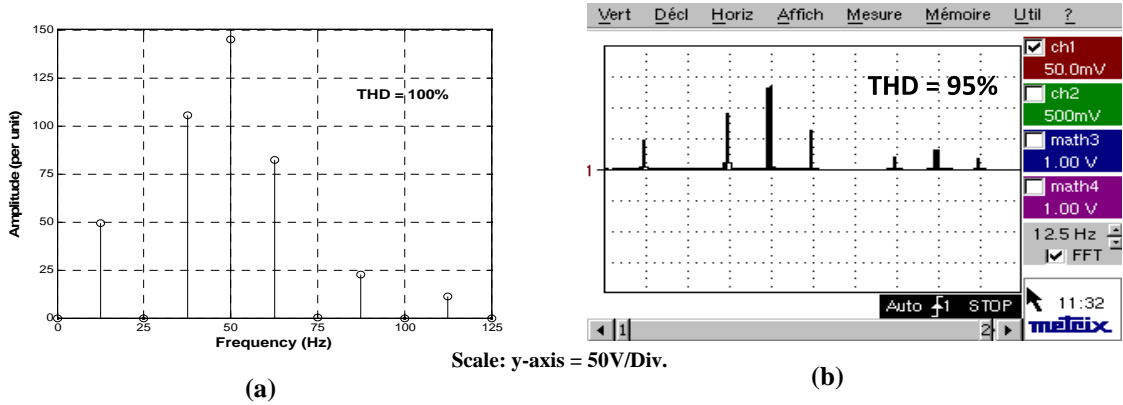

Fig.6 Schematic circuit diagram

Fig.7 Waveforms of signals at different points in the control circuit.

(a)

(b)

Voltage scale 400V/DIV. Time scale 10ms/DIV.

Fig. 8 Load voltages for $T = 4$ and $N = 2$, R load (a) before the correction (b) after the correction.

THD = 100%

(a)

THD = 95%

Scale: y-axis = 50V/Div.

(b)

Figure 9 Harmonic amplitude spectrum for (AM) $T = 4$ and $N = 2$, R load
(a) theoretically (b) practically.

		Table 2				
T	N	n_s (r.p.m.) before using shifting technique	Frequency of rotation (Hz) (Experimental)	n_s (r.p.m.) after using shifting technique	Frequency of rotation (Hz) (Experimental)	Frequency of the 1st harmonic (Hz) (Theoretical)
4	2	1914	31.9	760	12.6	12.5
4	3	2922	48.7	1006	16.8	12.5
5	2	2190	36.5	605	10.1	10
7	3	2455	40.9	480	8	7.1
7	4	2893	48.2	546	9.1	7.1
8	3	2534	42.2	369	6.15	6.2

The motor speed n_s is then measured at different values of load current (i_L) for $T = 4$ and $N = 2$ for both before and after correction cases of ψ_{nj}, the results are shown on curve1 and curve2 in Fig. 11 respectively. It is found that, the motor speed is reduced after the correction of ψ_{nj} and this is obvious since the motor rotates at the 1st harmonic frequency. The highest value of the load current shown on curve2 is less than that on curve1, this is because the generated e.m.f. in the dynamometer proportional to motor speed n_s, and any reduction in the speed leads to further reduction in the generated e.m.f. which in turn reduces the load current. Also any reduction in the value of the load resistance R in order to increase the load current at a certain value of V_{AH} leads to a reduction in the speed. This limitation in the loading machine performance does not allow us to take further readings to reach maximum loading of the motor.

V. Conclusion

The unbalanced sets of subharmonic and higher order harmonic voltages generated by integral cycle control technique create severe problems for ac machines as they found to cause excessive heat, mechanical vibrations and noise. Therefore, this type of control was abanded as an ac motor speed controller since many years ago. The proposed phase shifting technique in the present work is a try to solve the inherent limitation of this important type of control by shifting the second and third phases of the three-phase system by multiples of 2π. This technique is found to be more suitable than using the phase-angle control scheme to correct the unbalanced phase displacement angles of the generated harmonics. The last scheme is found to cause unbalanced

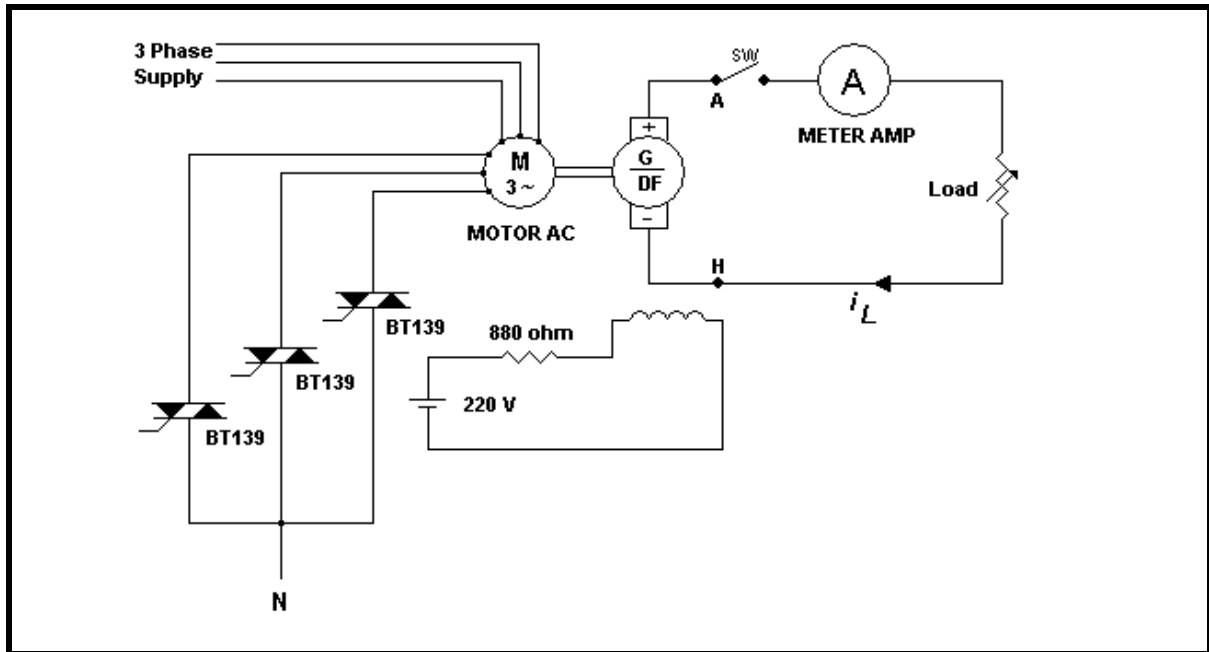harmonic amplitude spectrums for the three phases.

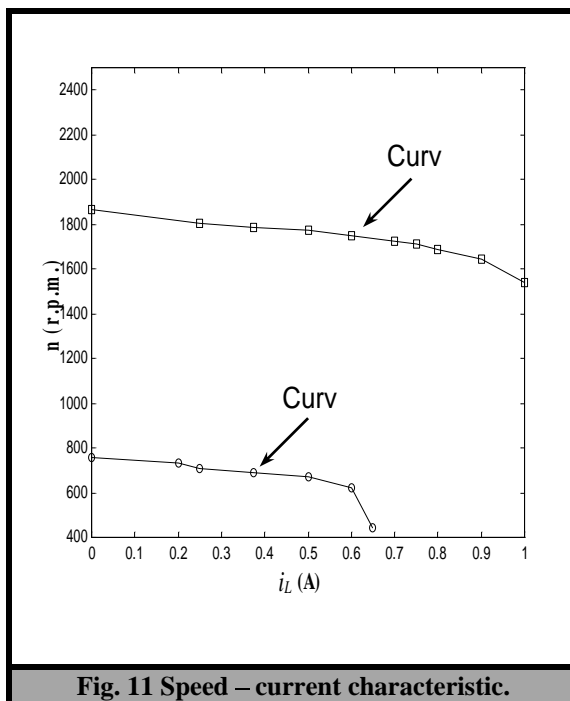**Fig. 10 Connection diagram for separately-excited dc dynamometer.**

Fig. 11 Speed – current characteristic.

It is found, from the theoretical and practical tests, that the performance of the three-phase induction motor with phase corrected voltage waveforms is very similar to that when fed from balanced sinusoidal voltages of the same amplitude and frequency when using the proposed phase-shifter. Finally, it is believed that the major problems associated with integral-cycle triggering control technique, when used for speed control of ac motor, have been solved in the present work.

Acknowledgments

Appendix A

The three − phase induction motor used to carry out the experimental investigation is a Elettronica Veneta (EV) demonstrating set (found in Machines laboratory, Electronic and Communications Department, Nahrain University). Other details of the motor are as follows:
P = 500W, V = 380VY / 220VΔ, I = 1.2A / 2.1A, n_s = 2850 r.p.m., frequency = 50Hz, No. of poles = 2

Appendix B

The machine used to carry out the experimental investigation is a Elettronica Veneta (EV) demonstrating set (found in Machines laboratory, Electronic and Communications Department, Nahrain University). The unit consists of a three − phase induction motor coupled to a dc dynamometer.
Other details of the motor are as follows:
P = 500W, V = 380VY/ 220VΔ, I = 1.4A / 2.4A, n_s = 2840 r.p.m., frequency = 50Hz, No. of poles = 2, $V_{rot.}$ = 365V, $I_{rot.}$ = 1.05A

While for the DC dynamometer
P = 450W, V = 220V, I = 2A at full-load, Exc. = SEP., $V_{exc.}$ = 220V, $I_{exc.}$ = 0.25A

Nomenclature

a_o	Zero order Fourier coefficient.
a_n, b_n	n^{th} order Fourier coefficients.
a_T, b_T	$n = T$ order Fourier coefficients.
c_n	Peak amplitude of nth Fourier harmonic.
c_T	Peak amplitude of Tth Fourier harmonic.
j	Integers, = 1, 2, 3
m_j	Integers, = 1, 2, 3, … , T-1
n	Order of harmonic.
n_S	Motor speed, r.p.m.
N	Number of conducting (on) cycles.
T	Control period = on + off cycles.
v_{Lj}	Load voltage at the jth phase, V.
V	Supply r.m.s. voltage, V.
ω	Angular supply frequency, rad/s.
ϕ	Phase-angle, rad.
ψ_n	Phase angle for n^{th} harmonic, rad.
ψ_T	Phase angle for T^{th} harmonic, rad.
γ_j	Phase displacement of the jth phase, rad.

References

[1] P. J. Gallagher, A. B. Barret, and W. Shepherd, "Analysis of single-phase rectified thyristor controlled load with integral-cycle triggering", *Proc. Inst. Elec. Eng.*, Vol.117, No.2, pp.409-414, Feb. 1970.

[2] B. W. Lingard, R. W. Johnson, and W. Shepherd, "Analysis of Thyristor Controlled Single-Phase Loads with Integral-Cycle Triggering", *Proc. Inst. Elec. Eng.,* Vol.117, No.2, pp.607-608, March 1970.

[3] P. J. Gallagher and W. Shepherd, "Operation of Two Parallel Connected Thyristor Controlled Resistive Loads with Integral-Cycle Triggering", *IEEE Transactions on Industrial Electronics and Control Instrumentation*, Vol. IECI-22, No.4, pp.510-515, 1975.

[4] W. Shepherd, "*Thyristor Control of ac Circuits*", Bradford University Press, England, 1975.

[5] M. Syed Jamil Asgher, "Fine Power Control by Discontinuous Phase-Controlled Switching", *IEEE Transactions on Circuits and Systems*, Vol.46, No.3, pp.402-405, March 1999.

[6] J. A. M. Chun Li and J. A. M.Wilsun Xu, "On the ambiguity of defining and measuring inter-harmonics," *IEEE Power Eng. Rev.*, pp. 56–57, July 2001.

[7] N. Mohan, T. Undeland, and W. Robbins, *Power Electronics*, 2nd ed. New York: Wiley, 1995.

[8] P. Krein, *Elements of Power Electronics*. New York: Oxford Univ. Press, 1998.

[9] R. Krishnan, B. Ilango, S. Selvarary, and S. Gunasekaran, "Single-Phase Induction Motor Speed Control with Integral-Cycle Switching", *IEEE Transactions on Industrial Electronics and Control Instrumentation*, Vol. IECI-27, No.4, pp.308-311, November 1980.

[10] N. H. Fetih, G. M. Abdel-Raheem, and G. A. Girgis, "Speed Control of a DC Series Motor Using an Integral-Cycle Controlled Single Traic", *IEEE Transactions on Energy Conversion*, Vol. 3, No. 3, pp. 618-623, September 1988.

[11] M. T. Lazim and W. Shepherd, "Analysis of Induction Motor Subjected to Nonsinusoidal Voltages Containing Subharmonics", *IEEE Transactions on Industry Applications*, Vol. IA-21, No.4, pp.956-965, July/August 1985.

[12] M. T. Lazim and W. Shepherd, "Three-Phase Circuits with Voltage Control by Integral-Cycle Single-Phase Mode Triggering of Thyristors", *IEEE Transactions on Industry Applications*, Vol.46, No.5, pp.507-520, September/October 1982.

[13] M. T. Lazim, "*Modulation Techniques in the Speed Control of Electric Motors*", Ph.D. thesis, University of Bradford, England, 1981.

[14] A. L. Mahmood, "*Microprocessor-Based Phase Shifter for Integral-Cycle Control*", M.Sc. thesis, Al-Nahrain University, Iraq, 2001.

[15] Yong Nong Chang, Gerald Thomas Heydt, and Yazhou Liu, "The Impact of Switching Strategies on Power Quality for Integral Cycle Controllers", *IEEE Transaction on Power Delivery*, Vol. 18, No. 3, pp.1073-1078, July 2003.

[16] Arifur Rahman, Syed Enamul Haque, and Ibrahim Abdul Rahman AL-Gadhi, "A Digital Self-Compensating Method for Integral-Cycle Power Control of *RL* Loads", *IEEE Transactions on Industrial Electronics and Control Instrumentation*, Vol. IECI-27, No.2, pp.49-53, May 1980.

[17] S. A. Nasar and L. E. Unnewehr, "*Electromechanics and Electric Machines*", John Wiley and Sons, Inc., 1979.

معدّل الطور للتوافقيات في نظام التضمين الموجي المتقطع

أ.م.د محمد توفيق لازم   د. أنس لطيف محمود

جامعة نهرين/ كلية الهندسة/ قسم الهندسة الالكترونية والاتصالات   جامعة فيلادلفيا /قسم الهندسة الالكترونية/ الأردن

الخلاصة:

يتضمن البحث إيجاد طريقة لتصحيح زوايا الطور غير المتوازنة للتوافقيات دون الأساسية وفوق الأساسية الناجمة عن استخدام إسلوب السيطرة بنظام تنظيم الموجة المتقطع او نظام حقن الدورات المتكاملة والتي تظهر عند تطبيق هذا النظام في الدوائر الثلاثية الطور حيث أن هذه المعضلة أدت إلى عدم استخدام هذا النظام الذي يمتلك خصائص جيدة في الأنظمة ذات الأطوار الثلاثة. تعتمد طريقة التصحيح على إزاحة الموجات للطور الثاني أو الثالث أو كلا الطورين معا بمضاعفات الدورة الكاملة.

تم تصميم وبناء نموذج أولي لمنظومة تصحيح الأطوار مختبرياً وتم فحص هذه المنظومة لأحمال تكونت من حمل مقاومي ومحرّك حثي ثلاثي الطور. لقد وجد بأن هنالك توافق جيد بين النتائج النظرية والعملية وفي رأي الباحث فإن المشاكل الرئيسية المصاحبة لأسلوب السيطرة بنظام الدورات المتكاملة للدوائر ثلاثية الأطوار والتي أدت إلى إنحسار استخدام هذا الإسلوب في السيطرة لسنين طويلة قد تم حلها في هذا العمل المقدّم.